TITLE

Multiple mechanisms mediate the suppression of motion vision during escape maneuvers in flying *Drosophila*.

AUTHORS

Philippe Fischer, Bettina Schnell

AFFILIATIONS

Emmy Noether Group Neurobiology of Flight Control, Max Planck Institute for Neurobiology of Behavior – caesar, Bonn, Germany

CORRESPONDING AUTHOR

Dr. Bettina Schnell
Max Planck Institute for Neurobiology of Behavior – caesar
Ludwig-Erhard-Allee 2
53175 Bonn
Germany

e-mail: bettina.schnell@mpinb.mpg.de

ABSTRACT

Animals must be able to discriminate self-generated (reafferent) from external (exafferent) sensory input. Otherwise, the former could interfere with perception and behavioral actions. The way this can be achieved is through an efference copy, which suppresses reafferent sensory input. An example for this is the optomotor response of the fly. With the optomotor response, flies stabilize a straight flight path by correcting for unintended deviations, which they sense as visual motion of their surrounding or optic flow. HS cells of the fly are tuned to rotational optic flow and are thought to mediate optomotor responses to horizontal motion. It has been shown that during spontaneous turns, an efference copy influences the membrane potential of HS cells. Here we investigate the influence of an efference copy during looming-elicited evasive turns combined with a subsequent optomotor stimulus in *Drosophila*. We show that looming stimuli themselves can influence the processing of preferred-direction motion in HS cells. In addition, an efference copy can influence visual processing during saccades in both directions, but only in a subset of cells. Our study supports the notion that processing of sensory information is finely tuned and dependent on both stimulus history and behavioral context.

INTRODUCTION

In a living organism, sensory perceptions do not exist in isolation, but are embedded into a context of internal state, other sensory stimuli and ongoing behavior. This holds true for vertebrates and insects alike, despite the manifest discrepancy in size of the CNS. Especially for flying insects, vision is an essential modality, to which a sizeable portion of their brain is dedicated. Illustrating the dependence on behavioral context, looming stimuli can signal an approaching predator or an impending collision. In stationary flies, they can elicit escape jumps, whereas in a flying fly they can trigger either a landing response or an evasive turn (Ache et al., 2019; Bender and Dickinson, 2006; von Reyn et al., 2014; Tammero and Dickinson, 2002b, 2002a). In addition, flies like vertebrates need to distinguish stimuli that are generated by their own behavior, such as motion of the surround, from external stimuli (Cullen, 2004; Von Holst and Mittelstaedt, 1950). In the optomotor response, for example, flies compensate for unintended deviations from a straight flight path, which they sense as motion of the surround or optic flow (Götz, 1968; Leonte et al., 2021; Mronz and Lehmann, 2008). However, this reflex-like compensation needs to be suppressed, when a fly performs a turn, which is also called a saccade. Saccades are rapid whole-body maneuvers that flies perform to change direction during flight (Muijres et al., 2014, 2015). Saccades do not only occur spontaneously, but can be triggered by looming stimuli, indicative of an impending collision or approaching predator (Bender and Dickinson, 2006; Heisenberg and Wolf, 1979; Tammero and Dickinson, 2002a). In head-fixed flight, they can be measured as fast changes in the difference between the left and right wing stroke amplitude (L-R WSA), which allows for studying their influence on visual processing in the fly brain (Heisenberg and Wolf, 1979; Maimon et al., 2010; Schnell et al., 2017). Saccades have been shown to follow a different motor program when executed spontaneously compared to when they are evoked by a looming stimulus (Dickinson and Muijres, 2016), but are indistinguishable in tethered flight quantified through changes in L-R WSA. In contrast to the large transients associated with saccades, the optomotor response is characterized by smaller changes L-R WSA, which increase with increasing duration of visual motion (Schnell et al., 2014).

HS cells are a class of large-field lobula plate tangential cells that respond to horizontal motion in a directionally selective fashion (Hausen, 1982b, 1982a; Schnell et al., 2010). They receive ipsilateral input from columnar motion detecting cells on their dendritic trees, but also contralateral input from other lobula plate tangential cells. There are three HS cells per hemisphere, HSN, HSE and HSS, which differ in the position of their dendritic trees in the lobula plate and thus their receptive fields (Schnell et al., 2010; Scott et al., 2002). Based on their response properties as well as activation and silencing experiments, they are thought to control stabilizing optomotor turns of the head and body during walking and flight (Busch et al., 2018; Fujiwara et al., 2017; Haikala et al., 2013; Kim et al., 2017). It has been shown that during spontaneous saccades an efference copy acts on HS cells, which has the appropriate sign to counteract responses to the visual stimulus that would be caused by the flies' self-motion (Kim et al., 2015, 2017). However, it remains unclear how this effect influences processing of large-field motion.

We studied how saccades influence visual processing in HS cells. To be able to time the execution of saccades, we used looming stimuli to trigger them and combined them with presentation of horizontal motion. Using whole-cell patch-clamp recordings during head-fixed flight (Joesch et al., 2008; Maimon et al., 2010; Schnell et al., 2014), we investigated, whether spontaneous and looming-elicited saccades have a similar effect on HS cells and whether this effect can indeed influence their processing of horizontal motion. In contrast to previous studies, we found a large variability between different HS cells regarding the influence of an efference copy during both spontaneous and looming-elicited saccades (Fenk et al., 2021; Kim et al., 2015, 2017). If present, the efference copy is able to inhibit responses to preferred direction horizontal motion in HS cells. In addition, we found that the looming

stimulus itself, when presented on the ipsilateral side, had a similar effect independent of the fly's behavior. Therefore, visual processing is not only influenced by an efference copy, but also by stimulus history.

RESULTS

To study the effect of an efference copy on the optomotor pathway, we recorded the membrane potential of HS cells from head-fixed flies during fictive flight, while monitoring turning behavior by measuring the difference between the left and right wing stroke amplitudes (L-R WSA) (Fig. 1) (Maimon et al., 2010; Suver et al., 2016). HS cells in the right optic lobe respond to rightward motion with a depolarization and to leftward motion with a hyperpolarization. We recorded from randomly selected HS cells from the right side of the brain only, whose dendritic receptive field is therefore on the right.

HS cell activity during saccades elicited by ipsilateral looming

To elicit turns, we presented a looming stimulus from either the left (contralateral) or the right (ipsilateral) side using an LED display (Fig. 1D). This stimulus mimicked an object approaching at a velocity of 1.5 m/s and was sufficient to elicit changes in L-R WSA. This change in L-R WSA likely corresponds to a free-flight saccade away from the stimulated side. In the following, we refer to these changes in L-R WSA as saccades, although the flies are not actually able to perform a turn in our preparation. Execution of saccades was variable meaning that flies did not always respond with a change of L-R WSA to the stimulus (Fig. 1E). We made use of this variability to test, whether an efference copy of the flies' behavior influences the membrane potential of HS cells similar to what has been reported for spontaneous saccades (Kim et al., 2015, 2017). We used a saccade detection algorithm on all trials from all flies to separate those with saccades from those without saccades (see Methods and Fig. S1) and averaged the HS cell membrane potential and L-R WSA across these two groups.

For looming stimuli presented on the right, which elicits a turn to the left, measured as decrease in L-R WSA (Fig. 2A), we did not find a difference in the average HS cell membrane potential between trials with and without a saccade (Fig. 2B). We did notice, however, that after the end of the stimulus presentation, when the looming stimulus disappeared, the membrane potential of the HS cells dropped rapidly and became slightly hyperpolarized independent of whether the flies performed a saccade or not.

HS cell activity during spontaneous saccades

It has been reported previously that spontaneous saccades to the left lead to a transient hyperpolarization of HS cells (Kim et al., 2015). We detected spontaneous saccades in our recordings using a similar algorithm as for the looming-elicited saccades, but limited to periods, during which visual stimuli were stationary (Fig. 2C). We confirmed that on average HS cells in the right hemisphere hyperpolarize during leftward saccades, although there was a lot of variability across cells with two HS cells even exhibiting a slight depolarization during the peak of the saccade (Fig. 2D). The variability is rooted in neither the detection efficiency nor the amplitude of saccades, given that flies with large saccades figure among the most depolarizing or hyperpolarizing cells.

To test whether spontaneous saccades had a different effect on HS cells than looming-elicited saccades, we sorted our recorded cells into two groups based on whether they exhibited a hyperpolarization during spontaneous saccades (HP_{spont} group, N=6) or no change in polarization (NP_{spont} group, N=5, omitting the depolarizing cells for now). Cells in the HP_{spont} group also showed a hyperpolarization during looming-elicited saccades (Fig. 2E), which is comparable to spontaneous saccades (Fig. 2G). This is the case despite changes in L-R WSA being larger during looming-elicited saccades. In the NP_{spont}

group there was no difference between trials with and without a saccade during the looming stimulus (Fig. 2F). These results indicate that a hyperpolarizing efference copy acts on only a subset of HS cells during both spontaneous and looming-elicited saccades.

Since the HP_{spont} and NP_{spont} subsets also respond differently to the looming stimulus itself (compare Fig. 2E and F), we hypothesized that they may correspond to different HS subtypes. There are three HS cells per hemisphere, which cover different parts of the visual field, and are called HSN (north → dorsal part), HSE (equatorial) and HSS (south → ventral part) (Fig S2A) (Fischbach and Dittrich, 1989; Schnell et al., 2010). However, for the majority of cells shown here, we did not obtain good intracellular dye fills and thus do not know the precise subtype. To test, whether the effect of an efference copy depends on subtype, we drew on data recorded in another context and extracted spontaneous saccades from them (Fig. S2B) (Schnell et al., 2014). Applying the same algorithm to this data with additional selection criteria, we obtained saccade-related-potentials in the absence of visual stimulation for 16 flies. Similarly to the case above, saccade-related potentials vary from hyper- to depolarization despite exhibiting strong saccades in a narrow range of amplitudes (Fig. S2C, D). However, results vary between subtypes. Prominently, all HSN cells hyperpolarized. In contrast, 3 out of 4 HSS cells exhibited a biphasic response with a weak hyperpolarization at saccade onset, followed by a depolarization that reached its peak just after the peak L-R WSA. HSE cell responses fall in between with some exhibiting a hyperpolarization and some a depolarization. Altogether, these data confirm the cell-to-cell variability, which can be explained by assuming that an efference copy during saccades has different effects on the different HS cell subtypes.

HS cell activity during saccades elicited by contralateral looming

To better distinguish the effect of a putative efference copy from the aftereffect of visual stimulation, we looked at looming stimuli presented on the left (contralateral) side, which elicits an increase in L-R WSA corresponding to a rightward saccade in most trials (Fig. 3A), and repeated the same analysis as described for ipsilateral looming. The membrane potential of the recorded HS cells became on average slightly hyperpolarized during trials with a saccade compared to trials without (Fig. 3B). This hyperpolarization occurred after the presentation of the stimulus, when the L-R WSA reached its peak. This hyperpolarization is also apparent, but less pronounced, when we average across trials with and without saccades for each fly individually and then plot the means across all flies (data not shown). Because most flies performed either many or only few saccades, though, this measure is more affected by noise. We also see the effect, when comparing trials from just one fly, suggesting that this is not simply due to variability between different flies (Fig. 1E). Thus, there is evidence that an efference copy influences the contralateral HS cell membrane potential during visually elicited saccades.

When looking at individual flies, we did not find the hyperpolarization during rightward saccades in all of the cells we recorded from. Rather, we were able to separate our recordings into two groups based on whether we were able to observe the effect (HP_{contra}) or not (NP_{contra}) (Fig. 3C). In four HS cells from four different flies we observed a clear hyperpolarization (Fig. 3D). In the other cells, we saw no clear difference in HS cell membrane potential between trials with and without a saccade (Fig. 3E). All HP_{contra} cells are also contained in the HP_{spont} group (see Table 1). We therefore suspect that here again these two groups represent different subtypes of HS cells (see also Fig. S2), which differ in the location of their dendritic tree and thus receptive fields.

The hyperpolarization we observed is different from the effect reported during spontaneous saccades. For spontaneous saccades, a depolarization has been reported during rightward turns (Kim et al., 2015). We also observed a slightly stronger depolarization during the presentation of the looming stimulus in trials with a saccade compared to those without (Fig. 3D), which occurred before L-R WSA started to rise. Because the depolarization could also be caused by the visual stimulus, however, we

cannot conclusively say, whether it is influenced by an efference copy or not. When we averaged the HS cell membrane potential during spontaneous saccades to the right of only the HP_{contra} group, we observed a similar hyperpolarization (Fig. 3F, G). This hyperpolarization is again preceded by a small depolarization suggesting that both are indeed the consequence of an efference copy. Altogether, there is no qualitative difference between the effect of spontaneous and looming-elicited saccades onto HS cells, although there is substantial cell-to-cell variability. In conclusion, for looming stimuli presented on the contralateral side, we did find evidence for a hyperpolarizing efference copy acting on a subset of HS cells.

Influence of looming-elicited saccades onto processing of horizontal motion stimuli

A major advantage of our approach, compared to studying spontaneous saccades, is that we can elicit the behavior and thus study its effect on a subsequent optomotor stimulus. To study, whether motion responses are altered in HS cells after a saccade, we presented a large-field horizontal motion stimulus directly after the looming stimulus, when the peak of the saccade occurred (Fig. 1D). Note that we chose stimulus parameters that are optimal for HS cells and thus slower than what flies would perceive during a free flight saccade. This stimulus consisted of random dots moving to either the left or the right. As a comparison, we measured responses to just the moving stimulus. A looming stimulus presented on the right triggers a saccade to the left, which during free flight would lead to rightward motion, which depolarizes the HS cells in the right optic lobe. While we did not find conclusive evidence for an efference copy during looming on the right side, we observed that the response to rightward motion after the looming stimulus was rising much slower when compared to the response to the motion stimulus presented alone (Fig. 4A, B). However, this is the case in flying as well as in resting trials. Further, the cells in the NP_{spont} group, which did not show any hyperpolarization to the looming stimulus (Fig. 2E), have a similarly suppressed motion response. (Fig. 4B). We therefore conclude that this suppression of the response to horizontal motion is a consequence of the looming stimulus itself presented on the side of the dendritic receptive field of the recorded HS cells and not of the flies' behavior. Therefore, in the case of an ipsilateral looming stimulus, an efference copy might not be necessary to suppress responses to large-field motion that could interfere with the execution of the saccade. However, in HP_{spont} cells (hyperpolarizing during saccades) the response to rightward motion is even further suppressed compared to resting, when the behavior is executed, showing that the presumed efference copy has an additional effect on motion processing (Fig. 4A).

For the looming stimulus presented on the left or contralateral side, we again plotted averaged responses separately for HP_{contra} cells (which showed the hyperpolarization) and NP_{contra} cells (which did not) (Fig. 4C,D). Here we found that responses to rightward motion were again rising much slower after a saccade compared to the response to just the motion stimulus, but only in the HP_{contra} cells where we found evidence for the hyperpolarizing efference copy, and only during saccades. Responses to leftward motion were not strongly affected (Fig. 4E, F). This finding suggests that the efference copy acting on HS cells during a contralateral looming stimulus serves to suppress responses to motion that would normally depolarize the cell. This finding is surprising given that a rightward turn should elicit predominantly leftward motion, which would hyperpolarize the cells.

DISCUSSION

We studied how neurons within the optomotor pathway in *Drosophila*, which corrects for deviations from a straight flight path, are influenced during (fictive) evasive turns elicited by looming stimuli. We found a complex dependence on cell type, behavior as well as the presence of a preceding visual stimulus. Excitatory responses to preferred-direction horizontal motion in HS cells are suppressed after looming stimuli on the ipsilateral side independent of the behavior. Thus, this suppression is likely mediated by the stimulus itself and not by an efference copy of the motor command controlling the

saccade, although the latter appears to play an additional role in a subset of HS cells. However, the effect does not depend on the response to the looming stimulus in itself. We can only speculate, whether this is a specific effect of the looming stimulus through a feedback mechanism or a consequence of light or motion adaptation in response to the dark disc. From an ethological perspective, there is very limited visual information to be expected in the same spot where an object rapidly approaches, such that unresponsiveness on that side might not be a disadvantage.

After a looming stimulus on the contralateral side, the suppression of excitatory responses in HS cells is only apparent in a subset of cells and dependent on the execution of a saccade and thus likely mediated through an efference copy. In contrast, hyperpolarizing responses to null-direction horizontal motion are not much affected by the preceding looming stimulus, although they have been shown to be able to elicit behavioral responses during walking (Busch et al., 2018). Generally, the effect of spontaneous saccades onto the HS cell membrane potential is not qualitatively different from the looming-elicited saccades for individual cells.

A recent study found evidence for an efference copy acting on HS cells during saccades elicited by looming stimuli presented on the ipsilateral side (Fenk et al., 2021). Fenk et al. did not report a similar variability between cells as our study, which is likely due to the fact that they only recorded from HSN cells. We found that HSE and HSS cells tend to be less or not hyperpolarized during spontaneous saccades to the left. Although our data on looming-elicited saccades did not discriminate between HS subtypes, the correlation between responses to spontaneous and looming-elicited saccades suggests that predominantly HSN receive an hyperpolarizing input also during escape saccades. Fenk et al. also did not study the effect of looming stimuli presented on the contralateral side. While we therefore confirm the results of their study, we find that the effect of both the stimulus as well as saccades onto HS cells collectively is more complex than previously reported.

A saccade during free flight is a complex maneuver consisting of a roll, a counter-roll and a yaw turn to realign the body with the new heading (Muijres et al., 2014, 2015). It is therefore difficult to judge, what the changes in L-R WSA correspond to. During free flight saccades, changes in L-R WSA were shown to be small and seem to have more impact on roll than on yaw torque, suggesting that the changes in L-R WSA we measure during tethered flight could correspond to the roll maneuver. It has been shown that during looming-elicited escape saccades in free flight the fly sacrifices stability for speed (Muijres et al., 2014, 2015). Spontaneous saccades on the other hand are more stereotyped and the yaw maneuver happens with smaller delay, such that times of motion blur are minimized (Land, 1999). The quantitative difference we find between spontaneous and looming-elicited saccades, might therefore be due to difference in the motor programs underlying these two behaviors. While a descending neuron has been described that is active during changes in L-R WSA associated with spontaneous as well as looming-elicited saccades (Schnell et al., 2017), it is still unclear, which neural substrate could mediate the efference copy.

What might explain the large cell-to-cell variability we observed regarding the effect of saccades on to HS cells? Because of the behavioral complexity, we do not know how the different types of HS cells would respond to the visual motion stimulus that would be caused by the fly's self-motion during a saccade. It is likely that the different types of HS cells because of their different receptive fields (Krapp et al., 2001; Schnell et al., 2010) could be differently influenced by this visual stimulus, which could explain why an efference copy seems to only act on some cells and not others. Our data are consistent with a model, in which HSN receives inhibitory and HSS excitatory input during saccades towards the contralateral side. Because of the electrical coupling between HS cells, HSE could receive indirect input via HSN and HSS with one or the other dominating in some cells, which could explain the response variability we observe in our recordings. In addition, there might be subtle differences in the behavior that we are not aware of, as we only measure L-R WSA. These differences in behavior could lead to

different effects onto HS cells. Further research is needed to disentangle the role that efference copies play in shaping neuronal responses during specific behavioral maneuvers. Efference copies and corollary discharge signals have been shown to influence sensory processing in a variety of different systems and at different levels culminating in the predictive coding hypothesis (e.g. Combes et al., 2008; Crapse and Sommer, 2008; França de Barros et al., 2022; Fukutomi and Carlson, 2020; Sommer and Wurtz, 2008; Wurtz, 2008). Despite decades of research, mechanisms for these phenomena remain speculative, and clarification could provide fundamental insights into the way nervous systems operate. Our study supports the notion that information processing already at early stages is strongly influenced by stimulus history as well as behavioral state. It is thus important when studying neuronal responses to consider the behavioral context.

MATERIALS AND METHODS

Resource availability

Further information and requests for resources and reagents should be directed to and will be fulfilled by the lead contact, Bettina Schnell (bettina.schnell@mpinb.mpg.de).

Fly stocks

Strains of *Drosophila melanogaster* were bred on premixed cornmeal-agar medium (JazzMix Drosophila food, Fisherbrand) at 25°C on a 12h day/12h night cycle. Flies used for experiments were of either wild-type CantonS (two flies) or expressing GFP in HS cells using the Gal4/UAS system (GMR81G07-GAL4 or GMR27B03-GAL4). All individuals had at least one wild-type allele for the *white* gene. To avoid side-effects of in-breeding, GMR27B03-GAL4; 2xUAS-EGFP flies were backcrossed to wildtype flies (Canton S and Top Banana), and offspring selected for fluorescence every few generations. We used female flies aged 2 to 5 days after eclosion for all experiments.

Electrophysiology

In vivo patch-clamp recordings of HS cells were performed in whole-cell configuration in current-clamp mode. Flies were anaesthetized on a cold-plate, legs amputated, and fixed by the head to custom-made pyramidal holders (Maimon et al., 2010) that allow access to portions of the head while offering free space to the wings using UV-curing glue. The head was bent forward to expose the posterior part in the surgery window of the holder. The head capsule was covered with extracellular saline (prepared according to Wilson and Laurent (Wilson and Laurent, 2005), in mM: 103 NaCl, 4 $MgCl_2$, 3 KCl, 1.5 $CaCl_2$, 26 $NaHCO_3$, 1 NaH_2PO_4, 10 Trehalose, 10 Glucose, 2 Sucrose and 5 TES, adjusted to 275 mOsm) and cut open using a syringe needle. The brain was perfused with extracellular saline bubbled with 95% O_2/5% CO_2 to reach pH 7.3. The neurolemma and extracellular matrix covering the lobula plate was digested by applying Collagenase (0.5mg/mL Collagenase IV in extracellular saline, Worthington) through a low-resistance pipette. HS cells were targeted under visual control with a 40x immersion objective (Nikon NIR Apo 40x/0.80W), phase-contrast filter, IR lighting (650 nm, Thorlabs) and CMOS camera (Thorcam Quantalux, Thorlabs), supported by short EGFP excitation in transgene flies. Patch pipettes were pulled with a P-1000 Flaming/Brown puller (Sutter Instruments) from thick-walled capillaries (Sutter instruments), adjusted to a resistance from 6 to 8 MΩ. Intracellular solution was prepared according to (Wilson and Laurent, 2005) (in mM: 140 mM potassium aspartate, 1 mM KCl, 10 mM HEPES, 1 mM EGTA, 4 mM MgATP, 0.5 mM NaGTP, 0.5% biocytin, adjusted to pH 7.3 and 265 mOsm) plus AlexaFluor-568. Signals were recorded with a BA-01X bridge amplifier (npi electronics) and a BNC-2090A digitizer (National Instruments) with MATLAB (version R2017b, The MathWorks). Recordings from HS cells presented in Fig. S2 were performed using the flies and setup described previously (Schnell et al., 2014).

Behavioral recordings

The flight behavior was observed by an IR-sensitive camera placed below the fly and illuminating the wings from the fly's posterior with the IR LED mentioned above. The front edge of the wing was detected in real time from the image stream using the Kinefly software (Suver et al., 2016) running on ROS (version Kinetic Kame), which outputs a signal that was fed into the same DAC together with the electrophysiological signal. An important change has been made to the Kinefly wing detection algorithm. The front edge of the wing was determined as the first threshold crossing of a derivative luminance signal extracted from the image.

LED arena and visual stimulation

The fly was at the center of a cylindrical arena of LED panels (IO Rodeo) as described (Reiser and Dickinson, 2008). Our arena is made of monochromatic LEDs (565 nm) where each pixel subtends an angle of 2.5 ° on the fly eye, covering a total visual field of about 195°x70°. Here, we used a frame shift rate of 50 Hz, while the arena was tuned to a flicker rate of about 744 Hz. The visual scene presented to the fly consisted of dark squares on a bright background. In fixed locations on either the left or right side, a dark disc expanded, simulating an object approaching at constant speed of 1.5 m/s. Thus the visual angle covered by the imaginary object is given by $\Theta(t) = 2arctan\left(\frac{-h}{vt}\right)$ with t<0 and t=0 at the expected moment of impact. To limit the angle to a maximum of 76.5°, we add a term t=t'+t_0 that offsets the angle when t' → 0. Setting h = 0.1 m and v = 1.5 m/s, t_0 ≈ -0.11s. Θ progresses from 2.25° to 60°. At time t' > 0, the looming disc disappears. The background is made of randomly distributed rectangles on a bright background, with each rectangle measuring at least 5° x 5° in the visual field. This background was rotated with a speed of 112.5 °/s for 240 ms to test the optomotor response either clockwise or counter-clockwise. In a given trial, the stimulus consisted in either looming (left/right) only, background rotation (either direction) only, or looming followed by background rotation, making for a total of 8 different stimulus combinations. Each trial lasted for 1.35 s, with an inter-trial interval of 3 s. The order of these stimuli was permuted, and overall repeated three times to complete one experiment run. Each fly completed several experiment runs.

Quality criteria

All data analysis was performed in Python (version 3.7). Recordings of HS cells were excluded if they did not respond to a square-wave pattern rotating counter-clockwise by a tonic hyperpolarization < -2 mV. All experiment runs for one fly were gathered and divided into trials, including 100 ms before and 250 ms after the actual trial. As a criterion for noisy trials we applied a threshold to the wing-stroke amplitude of both wings that was larger than the angle which the wing detection typically outputs in the case of misdetection (as artifacts of reflecting edges). This angle depended on preparation and light conditions, but in most instances is < 8° and is basically an angle that does not occur in normal flight. If both wings were consistently below threshold, the trial is classified as non-flying, and classified as flying if both wings were consistenly above threshold. If there was a discrepancy between left and right wing (above/below threshold) for more than 30 ms in a trial, corresponding to less than 2 detection frames, the trial was discarded. Spontaneous saccades were investigated by looking at the data from the inter-trial intervals, where the visual stimulus was static and consisted of the background only. In the older datasets (recorded as described in (Schnell et al., 2014)), the experiment files were truncated where resting membrane potential started to drift more than ≈ 0.01 mV/s .

Saccade detection

Saccades were detected using an algorithm based on continuous wavelet transform (CWT) applied to a differentiated signal. In a nutshell, any signal can be decomposed into a linear sum of many smaller wavelet functions which have a limited width in the time and frequency domains. An abrupt event of

significant amplitude shows in CWT as a time-localized peak over a broad range of wavelet scales. Thus it is detectable by tracking the uninterrupted peaks in the CW-transformed signal over scales. We use the algorithm developed by Du et al. (Du et al., 2006), as implemented in the scipy.signal (scipy version 1.6.2) package. First, to simplify saccade detection, we downsampled the noise-corrupted piece-wise-constant data obtained by recording the wing stroke amplitude together with electrophysiological data through a fitting procedure to obtain a single value per analysis frame. The downsampled signal was median-filtered with filter width 3 to remove single outliers, and then differentiated using the central difference formula with a half-width of 50 ms, to build the detection signal. This was fed into the peak-detection function with scales $\{2^{2+j/16}\}$, j = {0,2,…,15}, window size of 10, gap threshold of 1, and noise percentage of 5. To detect saccades to the left, the negative of the signal was used. Spontaneous saccades, where the direction of the saccade is not dictated by the stimulus, were detected in the same way on both the positive and negative signal with a window size of 20 and noise percentage of 10 to be more restrictive. For each putative saccade we calculated the peak and onset time and peak amplitude. The peak time was determined by moving forward from the putative peak and finding the first occurrence of crossing 0 in the signal used for detection and adding the half-width of the differentiation. The onset time was defined as the first minimum before the putative peak in the simple differential (not central difference) of the downsampled original signal. Peak amplitude was calculated by taking the average L-R WSA in the interval of peak time +/-30ms. To get rid of false positives, avoid cases of overlapping saccades, as well as the return to baseline after a previous saccade, we eliminated saccades if within the 160 ms preceding the onset existed a deviation from baseline, which exceeded a percentage of the peak amplitude. For spontaneous saccades, that percentage was 60%, while we chose 75% for saccades during looming trials. Trials were then classified according to whether they contained a saccade that was synchronized to the time when the looming stimulus reached its maximum expansion within a tolerance window of [-200 ms; 60 ms].

Additional filtering of putative saccades was applied to the data for different HS cell subtypes, shown in Fig. S2. First, a threshold was applied to the saccade amplitudes, tuned to one of {4.7, 7.4, 8.8, 11.8}°, with the two highest values by far the most common. Further, putative saccades were eliminated if the onset-to-onset interval between consecutive candidates of opposite direction was shorter than 500 ms or the deviation from onset exceeded 65% of amplitude during a window before onset of minimum. Finally a candidate saccade was accepted only if the onset preceded the peak in the (derivative) detection signal by at most 100 ms and the peak of the saccade followed by at most 300 ms. This procedure removes the vast majority of candidates, and the resulting putative saccades were visually verified in the context of the surrounding trace.

Analysis of electrophysiology data

Electrophysiology data in each trial was baseline-corrected to the mean potential in the window of 400 ms from the beginning of the trial. This window contains the background but very little visual motion. The data from trials was in principle averaged per fly, before calculating an average of averages with s.e.m. In cases where the low number of trials per fly in certain subsets did not allow computing a standard deviation, all trials were instead treated as coming from the same distribution, and therefore the mean ± s.d. was given. Which of these methods was applied is stated in the figure captions.

Criteria for subgroups

First, the difference in membrane potential before and after the maximum of the looming stimulus was calculated on the mean membrane potential for each fly for trials with looming stimulus only (no background rotation).

$$\mu_{before} - \mu_{after} = \mu[U(t|t \in [-140, -40]ms)] - \mu[U(t|t \in [+40, +110]ms)]$$

Flies were then grouped in the hyperpolarizing category if that difference was lower (more negative) than the average difference.

AUTHOR CONTRIBUTIONS

Conceptualization: B.S.; Methodology: P.F., B.S.; Software: P.F.; Formal Analysis: P.F.; Investigation: P.F., B.S.; Writing (Original Draft): P.F., B.S.; Writing (Review & Editing): P.F., B.S.; Visualization: P.F.; Funding Acquisition: B.S.; Supervision: B.S.; Project Administration: B.S.

COMPETING INTERESTS

The authors declare no competing interests.

ACKNOWLEDGMENTS

We want to thank Tim Krause for maintaining fly stocks, Gaia Tavosanis, Eugenia Chiappe and Michael Dickinson for sharing fly stocks and Elhanan Ben-Yishay and Kevin Briggman for comments on the manuscript. This work was funded by the German Research Foundation (DFG) through the Emmy-Noether program.

REFERENCES

Ache, J.M., Namiki, S., Lee, A., Branson, K., and Card, G.M. (2019). State-dependent decoupling of sensory and motor circuits underlies behavioral flexibility in Drosophila. Nat. Neurosci. *22*, 1132–1139.

Bender, J.A., and Dickinson, M.H. (2006). Visual stimulation of saccades in magnetically tethered Drosophila. J. Exp. Biol. *209*, 3170–3182.

Busch, C., Borst, A., and Mauss, A.S. (2018). Bi-directional Control of Walking Behavior by Horizontal Optic Flow Sensors. Curr. Biol. *28*, 4037-4045.e5.

Combes, D., Le Ray, D., Lambert, F.M., Simmers, J., and Straka, H. (2008). An intrinsic feed-forward mechanism for vertebrate gaze stabilization. Curr. Biol. *18*, R241–R243.

Crapse, T.B., and Sommer, M.A. (2008). Corollary discharge across the animal kingdom. Nat. Rev. Neurosci. *9*, 587–600.

Cullen, K.E. (2004). Sensory signals during active versus passive movement. Curr. Opin. Neurobiol. *14*, 698–706.

Dickinson, M.H., and Muijres, F.T. (2016). The aerodynamics and control of free flight manoeuvres in Drosophila. Philos. Trans. R. Soc. B Biol. Sci. *371*, 20150388.

Du, P., Kibbe, W.A., and Lin, S.M. (2006). Improved peak detection in mass spectrum by incorporating continuous wavelet transform-based pattern matching. Bioinformatics *22*, 2059–2065.

Fenk, L.M., Kim, A.J., and Maimon, G. (2021). Suppression of motion vision during course-changing, but not course-stabilizing, navigational turns. Curr. Biol. *31*, 4608-4619.e3.

Fischbach, K.F., and Dittrich, A.P.M. (1989). The Optic Lobe of Drosophila-Melanogaster. 1. A Golgi Analysis of Wild-Type Structure. Cell Tissue Res. *258*, 441–475.

França de Barros, F., Bacqué-Cazenave, J., Taillebuis, C., Courtand, G., Manuel, M., Bras, H., Tagliabue, M., Combes, D., Lambert, F.M., and Beraneck, M. (2022). Conservation of locomotion-induced oculomotor activity through evolution in mammals. Curr. Biol. *32*, 453-461.e4.

Fujiwara, T., Cruz, T.L., Bohnslav, J.P., and Chiappe, M.E. (2017). A faithful internal representation of walking movements in the Drosophila visual system. Nat. Neurosci. *20*, 72–81.

Fukutomi, M., and Carlson, B.A. (2020). A History of Corollary Discharge: Contributions of Mormyrid Weakly Electric Fish. Front. Integr. Neurosci. *14*, 42.

Götz, K.G. (1968). Flight control in Drosophila by visual perception of motion. Kybernetik *4*, 199–208.

Haikala, V., Joesch, M., Borst, A., and Mauss, A.S. (2013). Optogenetic Control of Fly Optomotor Responses. J. Neurosci. *33*.

Heinrich, R. (2002). Impact of descending brain neurons on the control of stridulation, walking, and flight in orthoptera. Microsc. Res. Tech. *56*, 292–301.

Heisenberg, M., and Wolf, R. (1979). On the fine structure of yaw torque in visual flight orientation of Drosophila melanogaster. J. Comp. Physiol. A *130*, 113–130.

Von Holst, E., and Mittelstaedt, H. (1950). The principle of reafference. Naturwissenschaften *37*, 464–476.

Joesch, M., Plett, J., Borst, A., and Reiff, D.F. (2008). Response properties of motion-sensitive visual interneurons in the lobula plate of Drosophila melanogaster. Curr.Biol. *18*, 368–374.

Kim, A.J., Fitzgerald, J.K., and Maimon, G. (2015). Cellular evidence for efference copy in Drosophila

visuomotor processing. Nat. Neurosci. *18*.

Kim, A.J., Fenk, L.M., Lyu, C., and Maimon, G. (2017). Quantitative Predictions Orchestrate Visual Signaling in Drosophila. Cell *168*, 280-294.e12.

Krapp, H.G., Hengstenberg, R., and Egelhaaf, M. (2001). Binocular contributions to optic flow processing in the fly visual system. J. Neurophysiol. *85*, 724–734.

Land, M.F. (1999). Motion and vision: why animals move their eyes. J. Comp. Physiol. A *185*, 341–352.

Leonte, M.-B., Leonhardt, A., Borst, A., and Mauss, A.S. (2021). Aerial course stabilization is impaired in motion-blind flies. J. Exp. Biol. *224*, jeb242219.

Maimon, G., Straw, A.D., and Dickinson, M.H. (2010). Active flight increases the gain of visual motion processing in Drosophila. Nat. Neurosci. *13*, 393–399.

Mronz, M., and Lehmann, F.-O. (2008). The free-flight response of Drosophila to motion of the visual environment. J. Exp. Biol. *211*, 2026–2045.

Muijres, F.T., Elzinga, M.J., Melis, J.M., and Dickinson, M.H. (2014). Flies evade looming targets by executing rapid visually directed banked turns. Science (80-.). *344*, 172–177.

Muijres, F.T., Elzinga, M.J., Iwasaki, N.A., and Dickinson, M.H. (2015). Body saccades of Drosophila consist of stereotyped banked turns. J. Exp. Biol. *218*, 864–875.

Reiser, M.B., and Dickinson, M.H. (2008). A modular display system for insect behavioral neuroscience. J. Neurosci. Methods *167*, 127–139.

von Reyn, C.R., Breads, P., Peek, M.Y., Zheng, G.Z., Williamson, W.R., Yee, A.L., Leonardo, A., and Card, G.M. (2014). A spike-timing mechanism for action selection. Nat. Neurosci. *17*, 962–970.

Schnell, B., Joesch, M., Forstner, F., Raghu, S. V, Otsuna, H., Ito, K., Borst, A., and Reiff, D.F. (2010). Processing of horizontal optic flow in three visual interneurons of the Drosophila brain. J. Neurophysiol. *103*, 1646–1657.

Schnell, B., Weir, P.T., Roth, E., Fairhall, A.L., and Dickinson, M.H. (2014). Cellular mechanisms for integral feedback in visually guided behavior. Proc. Natl. Acad. Sci. U. S. A. *111*, 5700–5705.

Schnell, B., Ros, I.G., and Dickinson, M.H. (2017). A Descending Neuron Correlated with the Rapid Steering Maneuvers of Flying Drosophila. Curr. Biol. *27*, 1200–1205.

Scott, E.K., Raabe, T., and Luo, L. (2002). Structure of the vertical and horizontal system neurons of the lobula plate in Drosophila. J. Comp. Neurol. *454*, 470–481.

Sommer, M.A., and Wurtz, R.H. (2008). Brain Circuits for the Internal Monitoring of Movements. Annu. Rev. Neurosci. *31*, 317–338.

Suver, M.P., Huda, A., Iwasaki, N., Safarik, S., and Dickinson, M.H. (2016). An Array of Descending Visual Interneurons Encoding Self-Motion in Drosophila. J. Neurosci. *36*, 11768–11780.

Tammero, L.F., and Dickinson, M.H. (2002a). The influence of visual landscape on the free flight behavior of the fruit fly Drosophila melanogaster. J. Exp. Biol. *205*, 327–343.

Tammero, L.F., and Dickinson, M.H. (2002b). Collision-avoidance and landing responses are mediated by separate pathways in the fruit fly, Drosophila melanogaster. J. Exp. Biol. *205*, 2785–2798.

Wilson, R.I., and Laurent, G. (2005). Role of GABAergic Inhibition in Shaping Odor-Evoked Spatiotemporal Patterns in the Drosophila Antennal Lobe. J. Neurosci. *25*, 9069 LP – 9079.

Wurtz, R.H. (2008). Neuronal mechanisms of visual stability. Vision Res. *48*, 2070–2089.

FIGURES

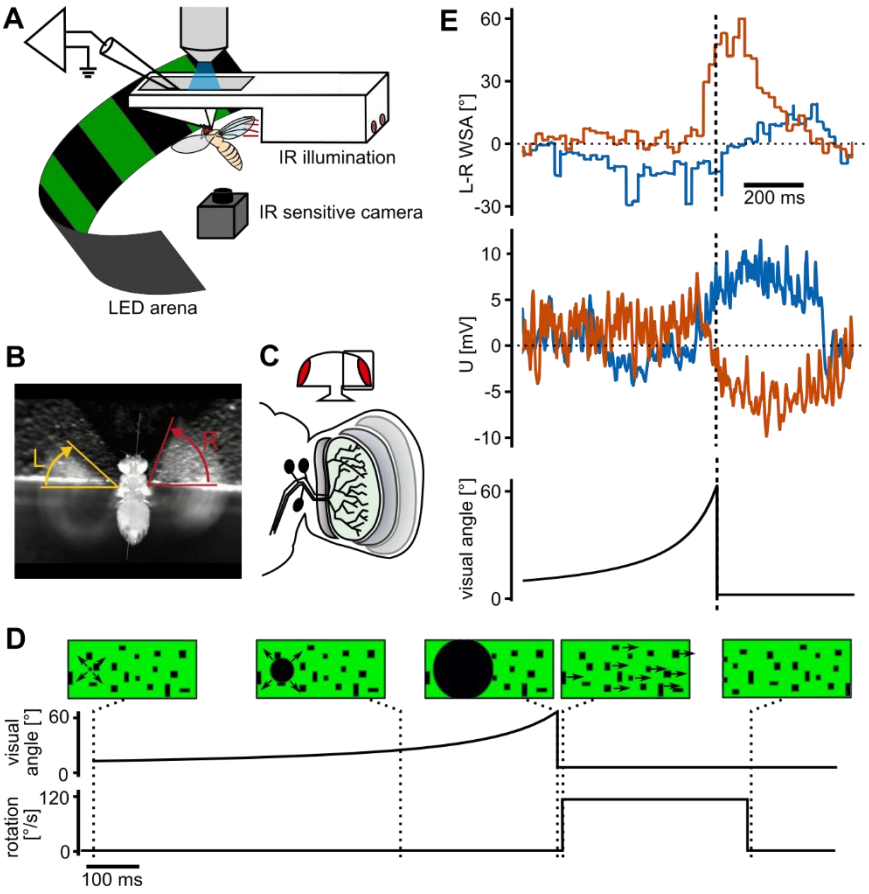

Figure 1

Whole cell recording of HS cells in flying *Drosophila* reacting to looming stimuli. (**A**) Schematic of the setup combining analysis of flight behavior under visual stimulation with whole-cell patch-clamp recordings in head-fixed *Drosophila*. (**B**) Example image of the video stream demonstrating the real-time analysis of wing stroke amplitude. (**C**) Schematic representation of the three HS cells located in the lobula plate within the optic lobe of the fly brain. (**D**) Visual stimulation protocol: a dark spot expands to a disc covering a large part of the visual field to simulate an object approaching at constant speed (looming stimulus) from either the left or right side. In Figure 4, this stimulus is immediately followed by a rotation of the whole field (called optomotor stimulus) to the left or right. (**E**) Example traces of behavioral response to looming from the left visual field from one fly. In many trials flies execute a rapid turn (saccade) away from the stimulated side (red trace, L-R >> 0 corresponds to a rightward turn). The same individual does not perform a saccade in other trials (blue). The membrane potential from a simultaneously recorded HS cells exhibit a hyperpolarization only during trials with a saccade. Saccades typically occur shortly before the looming disc reaches its maximal size.

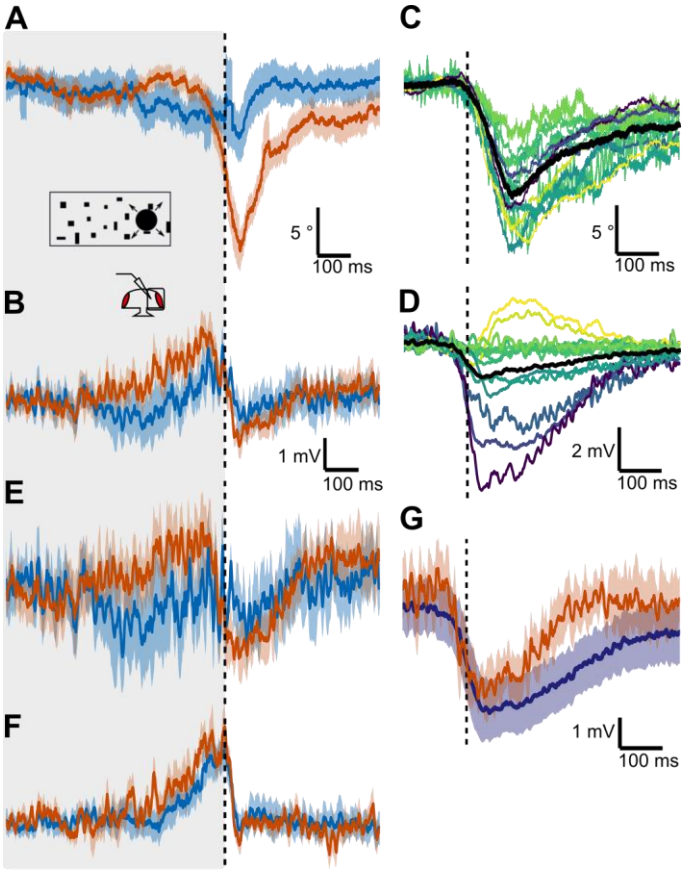

Figure 2

HS cell responses during looming-elicited saccades to the left. (**A**) Mean and SEM of L-R WSA of all flies in trials with looming stimulus presented on the right (ipsilateral) side separated into trials, where flies reacted with a saccade to the left (red) or not (blue), using a wavelet-based algorithm (see Methods). The dotted line marks the end of the looming stimulus. N = 13 flies. (**B**) Simultaneously recorded membrane potential of HS cells averaged across cells as in (A). One cell was recorded per fly. (**C**) L-R WSA during spontaneous saccades to the left for the same flies as in (A). Each color represents the mean of one fly. The population average in shown in black. (**D**) Mean change in HS cell membrane potential during spontaneous saccades corresponding to (C). (**E**) Membrane potential of a subset of cells selected based on their hyperpolarizing response during spontaneous saccades (HP_{spont}) (see D) from looming trials with an escape saccade (red, n = 25) or without a saccade (blue, n = 21) averaged across flies (N = 6 cells). (**F**) Average membrane potential of the remaining cells (NP_{spont} N = 5 cells) as in (E) (n = 28/33 trials). (**G**) Means of the cells that hyperpolarized during spontaneous saccades (peak voltage lower than 0, purple, N = 6 cells). As a comparison the responses of the same cells during looming-elicited saccades from (C) is replotted here (red).

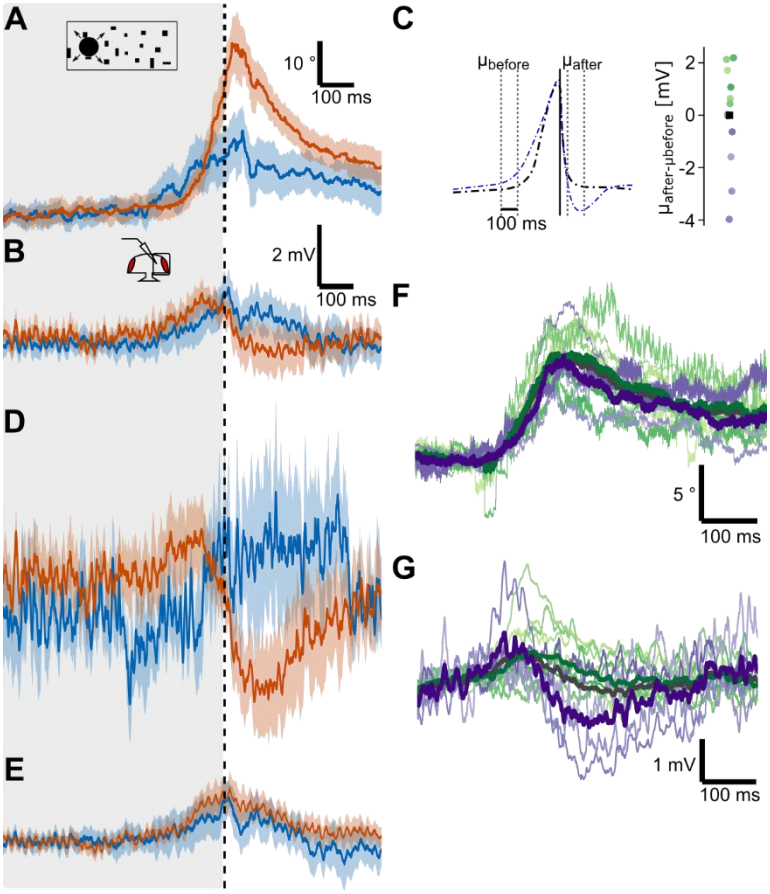

Figure 3

Evidence for a hyperpolarizing efference copy during looming-elicited saccades to the right in a subset of HS cells. (**A**) Mean L-R WSA in response to looming on the contralateral side (with respect to recorded cell) averaged across trials with a detected saccade (red, n = 74 trials) and those without (blue, n = 53 trials). N = 13 flies. (**B**) HS cell membrane potential corresponding to (A). One cell was recorded from each fly. (**C**) Criterion to split HS cells into groups according to their response to the looming stimulus during flight. The mean membrane potential after the stimulus is deducted from a baseline in the middle of the expansion (300 ms before maximal size). Flies are grouped by whether this difference is below (purple dots, HP_{contra}) or above average (green dots, NP_{contra}). (**D**) Membrane potential of the HP_{contra} subset of HS cells (purple cells from C, N = 4) for trials with (red, n = 23) and without saccades (blue, n = 8). Shown here is the average and standard deviation across all trials from all flies because of too few non-saccade trials per fly. (**E**) Same as (D), but for NP_{contra} cells (green dots from C, N = 9 flies). (**F**) L-R WSA during spontaneous saccades to the right for the same flies as in (A). Each color represents the mean of one fly. Thick lines represent averages across the different subsets according to (C) and across all flies (grey). (**G**) Membrane potential of HS cells during spontaneous saccades corresponding to (F).

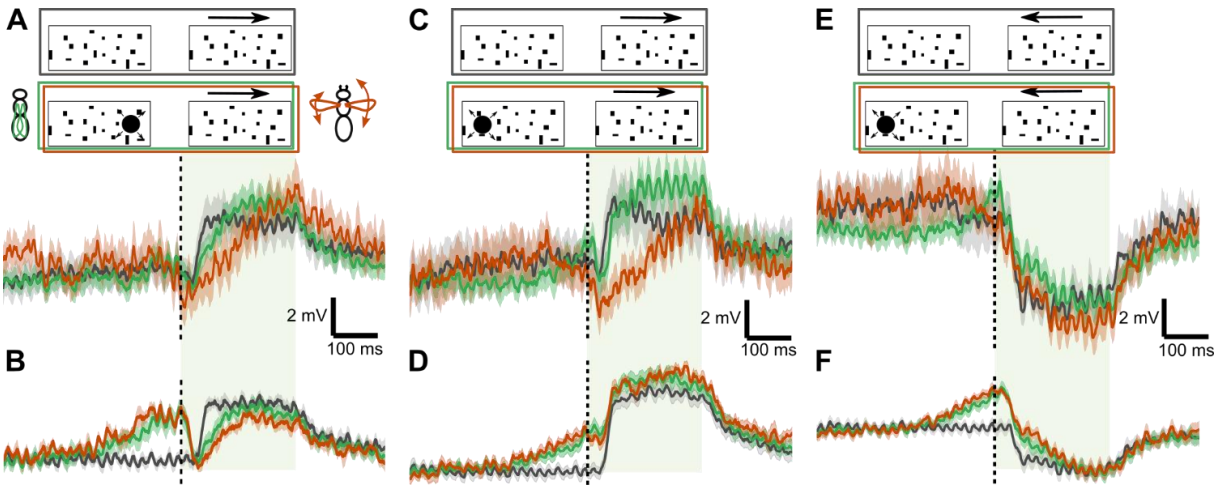

Figure 4

Processing of horizontal motion after a looming stimulus in HS cells. (**A**) Response to an excitatory (rightward) motion stimulus after a looming stimulus on the ipsilateral side of cells that hyperpolarize during saccades (HP_{spont}, same subset as in Fig. 2E). All traces represent mean ± s.e.m. membrane potential. Trials with saccades are shown in red, non-flight trials in green, optomotor stimulus without preceding looming stimulus in grey. (**B**) Same as (A), but for NP_{spont} (subset of HS cells that do not hyperpolarize, see Table 1 and Fig. 2D). (**C**) Response to an excitatory (rightward) motion stimulus after a looming stimulus on the contralateral side of cells that hyperpolarize during saccades HP_{contra} (same subset as in Fig. 3D). Color code as in (A). (**D**) Same as (C), but for NP_{contra} (subset of HS cells that do not show a hyperpolarization, see Fig. 3E). (**E**) Response to an inhibitory (leftward) motion stimulus after a looming stimulus on the contralateral side of HP_{contra} (same subset as in panel C). Color code as in (A). (**F**) Same as (E), but for NP_{contra} subset (same subset as in panel D).

TABLES

		Response to contralateral looming	
		HP_{contra} N=4	NP_{contra} N=9
Spontaneous Saccade related potential	HP_{spont} N=6	4	2
	NP_{spont} N=5	0	5
	depolarizing N=2	0	2

Table 1

Summary of classification of recorded cells according to their change in membrane potential during spontaneous saccades away from the ipsilateral side (HP_{spont}/NP_{spont}, see Fig. 2) and according to their response to a contralateral looming stimulus (HP_{contra}/NP_{contra}, see Fig. 3). Groups are highly concurrent, with HP_{contra} being a subset of HP_{spont} and NP_{spont} a subset of NP_{contra}. HP = hyperpolarized, NP = no change in polarization.